Article

Chain-Length Effects on the Self-Assembly of Short 1-Bromoalkane and *n*-Alkane Monolayers on Graphite

Gina M. Florio, Tova L. Werblowsky, Boaz Ilan, Thomas Mu#ller, B. J. Berne, and George W. Flynn

J. Phys. Chem. C, **2008**, 112 (46), 18067-18075 • DOI: 10.1021/jp8064689 • Publication Date (Web): 28 October 2008

Chain-Length Effects on the Self-Assembly of Short 1-Bromoalkane and *n*-Alkane Monolayers on Graphite

Gina M. Florio,*,† Tova L. Werblowsky,‡,§ Boaz Ilan,‡,∥ Thomas Müller,‡,⊥ B. J. Berne,*,‡ and George W. Flynn‡

Department of Chemistry and Department of Physics, St. John's University, Queens, New York 11439, and Department of Chemistry and the Columbia Center for Electron Transport in Molecular Nanostructures, Columbia University, New York, New York 10027

Received: July 22, 2008; Revised Manuscript Received: September 9, 2008

The structural properties of self-assembled monolayers of short 1-bromoalkanes and *n*-alkanes on graphite were investigated by a combination of ultrahigh vacuum scanning tunneling microscopy (UHV-STM) at 80 K and theoretical methods. STM images of 1-bromohexane reveal a lamellar packing structure in which the molecules form a 57° ± 3° lamella-molecular backbone angle and a head-to-head assembly of the bromine atoms (Müller, et al. *Proc. Natl. Acad. Sci. U.S.A.* **2005**, *102*, 5315). STM images of 1-bromoheptane also show a head-to-head 60° ± 3° lamella-molecular backbone pattern; however, the molecules pack in a herringbone structure. The odd/even chain-length alternation in the monolayer morphologies of 1-bromoalkanes is similar to that observed for the self-assembly of short *n*-alkanes on graphite, suggesting that the bromine atom acts effectively as an extension of the carbon backbone. The analogy, however, is incomplete. Odd and even short *n*-alkanes (hexane, heptane, octane) display 60° herringbone and rectangular (not 60°) lamella-molecular backbone configurations, respectively. The balance of intermolecular forces and packing considerations responsible for this odd/even alternation in monolayer morphology for short 1-bromoalkanes on graphite is examined here according to classical molecular dynamics simulations and in light of the structural properties of analogous *n*-alkane assemblies.

Introduction

The self-assembly of functionalized organic molecules at interfaces is governed by an intricate balance of adsorbate−substrate and adsorbate−adsorbate interactions. The ability to dissect these interactions would enable *a priori* design of 2D structural patterns,[1] which is expected to influence the design of functional nanometer scale materials. Simple *n*-alkanes and their derivatives serve as ideal model systems upon which to study the interplay of molecular forces responsible for self-assembly. Scanning tunneling microscopy (STM) is well suited to the task of revealing the atomic scale details of the self-assembly process. The spontaneous ordering of organic molecules, particularly of *n*-alkanes and their derivatives has been studied extensively using STM at the liquid−solid interface. Seminal initial studies[2−6] and numerous informative reviews are available.[1,7−15] More recently, STM studies of simple *n*-alkane derivatives have been performed at the vacuum−solid interface.[16,17] The vacuum environment further simplifies the analysis by eliminating adsorbate−solvent interactions. Solvent is expected to modify the potential energy landscape by lowering barriers between different structural minima and by opening new dynamic pathways.[18−21] Even the presence of one-third of a solvent layer atop an *n*-alkane monolayer is known to alter the interfacial structure.[22] The modeling of monolayer structures on graphite surfaces using theoretical methods for energy minimization and molecular dynamics simulations allows intermolecular and absorbate-substrate forces to be partitioned into classical force field contributions such as electrostatic, dispersion, and image charge interactions.[17,23−28] As such, subtleties of the self-assembly can be explored systematically with an emphasis on the role of molecular structure and functionality.

The adsorption, structure, melting behavior, and dynamics of *n*-alkane films on graphite have been widely investigated using a variety of additional techniques, including thermodynamic,[29−33] X-ray and neutron diffraction,[22,34−46] low-energy electron diffraction,[40] and theoretical methods.[27,38,47−61] Diffraction studies of short *n*-alkane (≤16 carbons) monolayers reveal an odd/even alternation such that the even-length *n*-alkanes form herringbone assemblies belonging to the 2D space group *cm*,[46] while odd ones form rectangular lamella-molecular backbone structures belonging to *pgg*.[45] Odd/even alternations in morphology are also observed for longer *n*-alkanes; however, the morphologies are of the rectangular (odd) or oblique (even) type.[34] The odd/even structural changes observed in the *n*-alkanes in 2D have been identified as the possible origin of the alternation in the melting point and dynamics of the corresponding monolayers.[62]

Odd/even effects are also observed in monolayer films of simple *n*-alkane derivatives. Short 1-alcohols with seven carbon atoms or less exhibit odd/even effects in their melting phase transitions,[63−65] despite the gross similarity in their monolayer structures. Both odd and even n-alcohols form herringbone

* To whom correspondence should be addressed. Phone: (718) 990-2638 (G.M.F.); (212) 854-2186 (B.J.B.). Fax: (718) 990-1876 (G.M.F.); (212) 854-7454 (B.J.B.). E-mail: floriog@stjohns.edu (G.M.F.); bb8@columbia.edu (B.J.B.).

† St. John's University.

‡ Columbia University.

§ Current address: Department of Chemistry and Physics, Touro College, New York, NY 10010.

∥ Current address: Schrödinger, LLC, 120 W. 45th Street, New York, NY 10036.

⊥ Current address: Veeco Metrology Group, 112 Robin Hill Rd., Santa Barbara, CA 93117.

10.1021/jp8064689 CCC: $40.75
Published on Web 10/28/2008

patterns in which the polar hydroxyl groups are oriented in a head-to-head assembly to facilitate hydrogen bonding. The microscopic origin of the alternation in the melting behavior is thought to be associated with differences in dynamics due to the orientation of the terminal methyl group cis (even) or anti (odd) with respect to the hydroxyl group and the resultant tight (even) or loose (odd) packing among chains.[63] Alkanoic acids[66−70] also exhibit odd/even alternation in their melting as well as their 2D assembly structures.

Of fundamental interest in the field of molecular self-assembly is the relationship between the structure of the 2D crystallites formed on solid supports and the 3D pure crystals. The structure of the monolayer can be used, for example, to direct the growth of 3D crystals via heterogeneous nucleation. For odd/even intermediate length *n*-alkanes,[34] as well as *n*-alcohols,[71] distinct surface structures are observed on graphite that differ from the pure 3D crystals, as well as bulk crystals grown on graphite. The presence of the substrate clearly alters the crystallization due to the strength of the interaction between alkyl chains and the graphite lattice.

The monolayer self-assembly of halogen substituted *n*-hexanes, including 1-bromohexane, has recently been investigated using a combined STM and theoretical approach.[17] The electrostatic and dispersion energy associated with the halogen, while small in magnitude relative to the total potential energy of the system, strongly influences the resultant packing structure. The molecules align with their bromine groups in a head-to-head configuration characterized by a 60° angle between the lamella and molecular backbone axes. Here we extend our previous study by exploring the effect of chain length on packing in comparing the morphologies formed by 1-bromohexane with those formed by 1-bromoheptane at the vacuum-graphite interface. In addition, we provide STM images of monolayers formed by hexane, heptane, and octane on graphite under vacuum in support of structural analysis by diffraction experiments.[45,46] These *n*-alkanes systems serve also as reference for understanding the odd/even effect for short bromoalkanes. Likewise, experiment and theory are linked by utilizing the most idealized experimental conditions, namely, ultrahigh vacuum (UHV). The chains were chosen to be sufficiently short (<10 carbons) to ensure an appreciable effect of the functionalized endgroups on the observed mophologies.

This study presents a previously unreported odd/even packing alternation for short 1-bromoalkanes analogous to short *n*-alkane monolayers on graphite. The odd (even) 1-bromoalkanes act as even (odd) *n*-alkanes since the terminal bromine atom serves as an extension of the carbon backbone. 1-Bromoheptane, with seven carbon atoms and one bromine atom, displays the same herringbone morphology observed for the even-length *n*-alkane monolayers of hexane and octane. Similarly, 1-bromohexane, like the odd-length *n*-alkane heptane, does not form herringbone morphologies. The lamella-backbone angle of 1-bromohexane (∼60°) is, however, different than that of its analogue odd-length *n*-alkanes (90°). A related odd/even packing alternation is observed for 1-bromodocosane ($C_{22}H_{45}Br$),[5] 1-bromoeicosane ($C_{20}H_{41}Br$),[72] and 1-bromononadecane ($C_{19}H_{39}Br$).[72] It is thought that the stability of the 60° over the 90° lamella-backbone angle for 1-bromoeicosane under vacuum is due to the dipole moment of the C−Br headgroup[17] and a very narrow basin for the potential energy surface about the energy minimum of the 90° morphology.[21]

The primary driving force for molecular self-assembly is the ability of the molecules to cover the surface efficiently, thereby lowering the total potential energy of the system. Indeed, analysis of a two-dimensional structural database (2DSD) compiled by Matzger and co-workers[1] provides unequivocal evidence for the principle of close-packing as the primary driving force in surface ordering. Furthermore, the details of the surface morphology are also determined by an intricate balance of intermolecular forces. It has been suggested that the relative orientation of the terminal methyl groups governs the observed packing structures of the short *n*-alkanes in 2D by minimizing the steric interactions across lamellae.[31,69,73,74] The present work provides further evidence in support of this interpretation. In addition, these results suggest that the relative orientation of the terminal methyl groups effects the optimal coverage of *n*-alkanes on the graphite surface.

Methods

STM experiments were conducted under ultrahigh vacuum (UHV) at a base pressure of 1×10^{-10} torr. The UHV chamber was equipped with a variable temperature STM (Omicron), along with other surface analysis instrumentation. Highly oriented pyrolytic graphite, HOPG, (GE Advanced Ceramics, *ZYB* grade) was freshly cleaved prior to immediate introduction into the vacuum system. The HOPG was cleaned by annealing to 820 K for ∼20 min prior to cooling for deposition of molecular adsorbates.

1-Bromohexane, 1-bromoheptane, hexane, heptane, and octane are liquids at room temperature with high enough vapor pressure to be vapor deposited onto the HOPG substrate held between 135 and 180 K. All samples were obtained from Aldrich (>98%) and purified by a minimum of ten freeze−pump−thaw cycles prior to use. Vapor deposition was performed in the STM stage of the UHV chamber using a retractable line-doser aimed at the cold HOPG substrate with the STM tip fully retracted. In general, ∼5−10 L of the sample was deposited. Guided by the results of previous temperature-programmed desorption[31,32] and STM studies,[17]substrate temperatures during dosing were chosen to permit monolayer formation while ensuring rapid desorption of multilayers. Both 1-bromoalkanes were dosed at substrate temperatures of 180 ± 5 K. The *n*-alkanes were dosed at substrate temperatures ranging from 135−150 K. Despite the fact that the deposition temperatures used for the *n*-alkanes are below their melting temperatures, 170 K for hexane,[38] the monolayers are known to be dynamic and undergo rotator phases at or near the deposition temperatures.[38,49,57,59,60] To our knowledge, there are no analogous data for 1-bromoalkane monolayers in the literature. After dosing, the substrate temperature was lowered at a rate of <0.1 K/s to 75−80 K for imaging. Both the deposition temperatures and slow cooling should be sufficient to avoid trapping the monolayers in higher energy configurations.

STM tips were prepared by electrochemical AC etching of a polycrystalline tungsten wire. All images were acquired in constant current mode. Typical scanning conditions are +2 V bias between the tip and the surface, 100 pA tunneling current, and a scan rate of 6−8 lines/s. The effects of thermal and mechanical drift were often minimized through use of the real-time drift correction feature available in the Omicron imaging software. Specific tunneling parameters are given for individual images in the figure captions, with the sign of the voltage referenced to the sample.

Theoretical analysis of the self-assembled monolayers at the vacuum-graphite interface was performed according to a previously described methodology.[17,23,24,26] Briefly, energy minimization and molecular dynamics were performed using the SIM[75] Molecular Dynamics package. The Truncated Newton Algo-

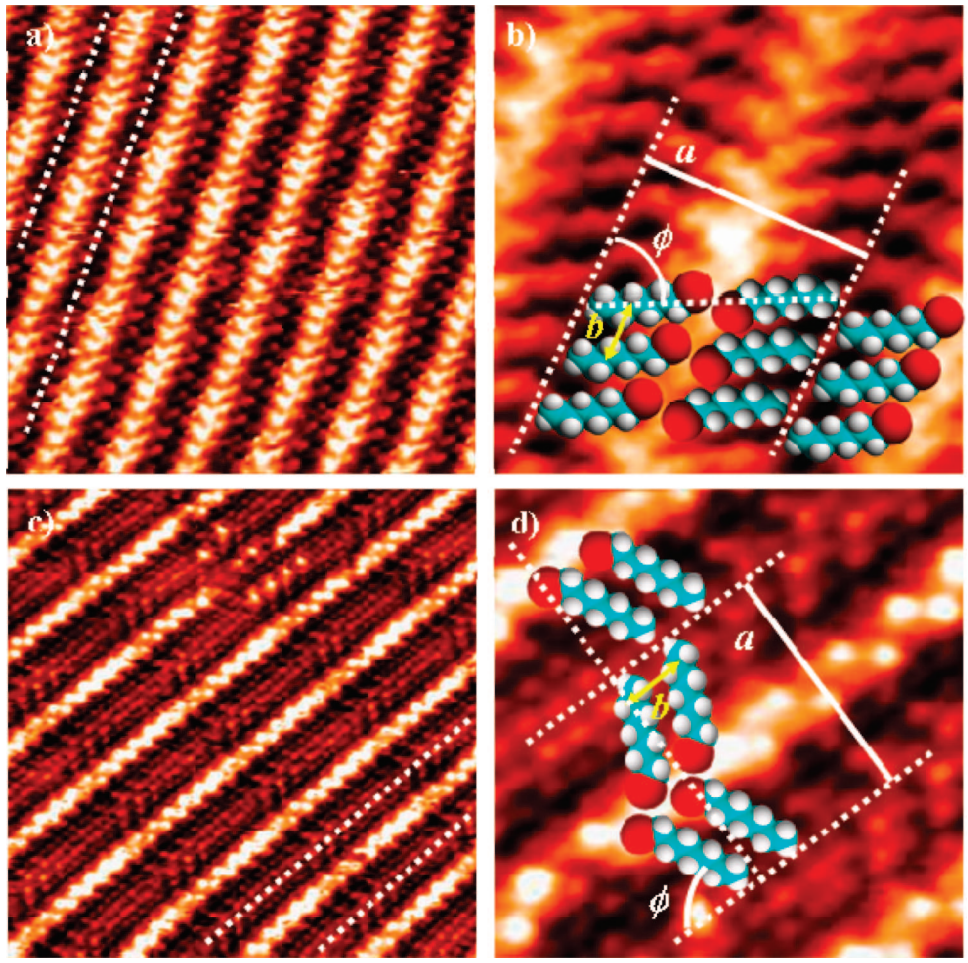

Figure 1. UHV STM images of 1-bromoalkanes on graphite at 80 K. (a) 1-bromohexane (BrC_6) at 14 nm × 14nm, +2.0 V, 200 pA (b) BrC_6 at 4 nm × 4 nm, +2.0 V, 200 pA (c) 1-bromoheptane (BrC_7) at 14 nm × 14 nm, +1.8 V, 100 pA, active drift control, and (d) BrC_7 at 4 nm × 4 nm, +1.9 V, 100 pA, active drift control. White dotted lines indicate the double lamella width, and other structural parameters are identified. All images have been FFT filtered slightly to sharpen features without inducing distortion. A defect in the BrC_7 self-assembly pattern can be seen at the top center of Figure 1c.

TABLE 1: Structural Parameters Measured for the 1-Bromoalkane Monolayers on Graphite and Their Corresponding Energy Minimized Structures

molecule	lamella spacing (a)[a]	perpendicular intermolecular distance ($b_\perp$)[b]	lamella-backbone angle (ϕ)[c]
1-bromohexane STM	1.73 ± 0.01 nm	0.44 ± 0.03 nm	57° ± 3°
1-bromohexane Theory	1.72 ± 0.02 nm	0.44 ± 0.03 nm	60° ± 3°
1-bromoheptane STM	1.82 ± 0.01 nm	–	60° ± 3°
1-bromoheptane Theory	1.84 ± 0.02 nm	0.44 ± 0.01 nm	61° ± 1°

[a] The lamella spacing (a) defined in Figure 1 corresponds to the projection by sin ϕ of the length of two 1-bromoalkane molecules associated in a head-to-head arrangement. [b] The intermolecular distance measured perpendicular to the molecular axis ($b_\perp$) is given by $b_\perp = b \sin \phi$ where b is the intermolecular distance measured along the lamella axis (Figure 1). [c] The lamella-molecular backbone angle, (ϕ) in Figure 1.

rithm[76] in combination with extensive simulated annealing runs were used to locate the global minimum of the potential energy for the different morphologies. Such extensive sampling is also required to eliminate the possibility of local minima in the torsion potential energy. Torsionally trapped minima could play a role in minimization calculations, since *gauche* defects may be present statically at grain boundaries for larger systems.[61] Constant temperature molecular dynamics (MD) simulations were performed according to the Nose−Hoover chains method[77] to mimic experimental conditions. The interactions of the graphite lattice with the adsorbate molecules were modeled using the pairwise Lennard-Jones potential according to the Steele form.[78−80] The graphite lattice was modeled as two fully corrugated layers on top of 38 noncorrugated layers. The adsorbate intramolecular and intermolecular energetics were described using Jorgensen's OPLS all-atom force field.[81] Intramolecular energy is described by harmonic bond stretches, bends, and torsions, as well as by Lennard−Jones (6−12) dispersions and repulsions, and electrostatic interactions between atoms separated by at least three bonds (1−4 interactions). Intermolecular energy is described by electrostatic interactions (point charges) and Lennard−Jones (6−12) dispersion interactions. In addition, image charge interactions between the molecules and the substrate were included in the model.[21] Periodic boundary conditions were not imposed since the application of the Steele potential restricts the lengths of the simulation box to be an integer multiple of the graphite periodicity. Nonperiodic patches of 16 bromoalkane molecules

were examined on the model graphite substrate. While such a system size suggests the possibility of systematic errors due to edge effects, a larger system would likely accumulate registry errors since the OPLS force field has not been reparameterized with respect to the graphite lattice. In addition, it could be argued that such edge effects cancel when comparing different morphologies, especially when they belong to the same symmetry class. Alternatively, a smooth model of the graphite surface could be used to include periodic boundary conditions in the monolayer simulations.[24] The theoretical studies rationalize the preference of one monolayer formation over another under experimental conditions, and we expect the magnitude of the edge effects to be similar for all monolayer structures examined (see Figure 2).

Results

Representative UHV-STM topographic images of monolayers of 1-bromohexane[17] (BrC_6) and 1-bromoheptane (BrC_7) formed on the basal plane of graphite are shown in Figure 1. Upon extensive investigation, only one type of packing morphology was observed for each monolayer film. The STM images reveal important qualitative and quantitative structural information about these self-assembled monolayers. STM topographs for the BrC_6 (Figure 1a, b) and BrC_7 (Figure 1c, d) monolayers show that both molecules form highly ordered arrays on graphite. The double lamella width is indicated by the dashed white lines. Bromine end-groups appear as bright protrusions while the alkyl chains are less bright. The structural parameters measured from the STM images are displayed in Table 1.

STM images of BrC_6 on graphite (Figure 1a, b) indicate that the molecules form a head-to-head, angled assembly pattern as shown by the properly scaled molecular model overlay in Figure 1b. The bright stripe down the middle of the lamella indicates the position of the bromine atoms. The lamella-backbone angle (ϕ) is $57 \pm 3°$, the lamella spacing (a) is 1.73 ± 0.01 nm, and the intermolecular distance measured along the lamella axis (b) is 0.53 ± 0.02 nm (Figure 1b). The intermolecular distance measured perpendicular to the molecular backbone ($b_\perp = 0.44 \pm 0.03$ nm) is defined according to $b_\perp = b \sin \phi$. The length of a single BrC_6 molecule is calculated to be 0.87 nm. As expected, the double lamella spacing (a) is essentially the projection by $\sin \phi$ of twice the length of a single molecule, including the van der Waals diameter of a carbon atom to account for the trough width. In keeping with previous studies of alkanes on graphite, length measurements indicate that individual molecules lie with their backbones in the energetically favorable all-*trans* configuration.[4,11,82] The intermolecular distance ($b_\perp = 4.4$ Å) is slightly larger than that required for commensurate epitaxy with the graphite lattice (4.26 Å), and as such, Moiré patterns are observed along the lamella axis. Slight mismatches between the length of carbon−carbon bonds of the alkyl chains and those of the substrate also result in noncommensurate packing laterally. This was confirmed via STM imaging using a very large gap resistance. Energy minimizations and molecular dynamics simulations for BrC_6 monolayers on a model graphite surface are in good agreement with the two-dimensional crystallographic parameters determined via STM (Table 1).

The STM images do not allow us to determine the exact orientation of the terminal bromine atom. According to the theoretical analysis, the bromine atoms lie in the same plane as the carbon backbone and effectively become an extension of the alkyl chain. From the calculations, the approximately fixed distance between the Br atom and the graphite surface is due to the large value of its Lennard−Jones ε parameter which is a factor of ~7 and 16 larger than that of carbon and hydrogen, respectively. This translates into a deep potential well for the dispersive interactions between Br and all other atoms and

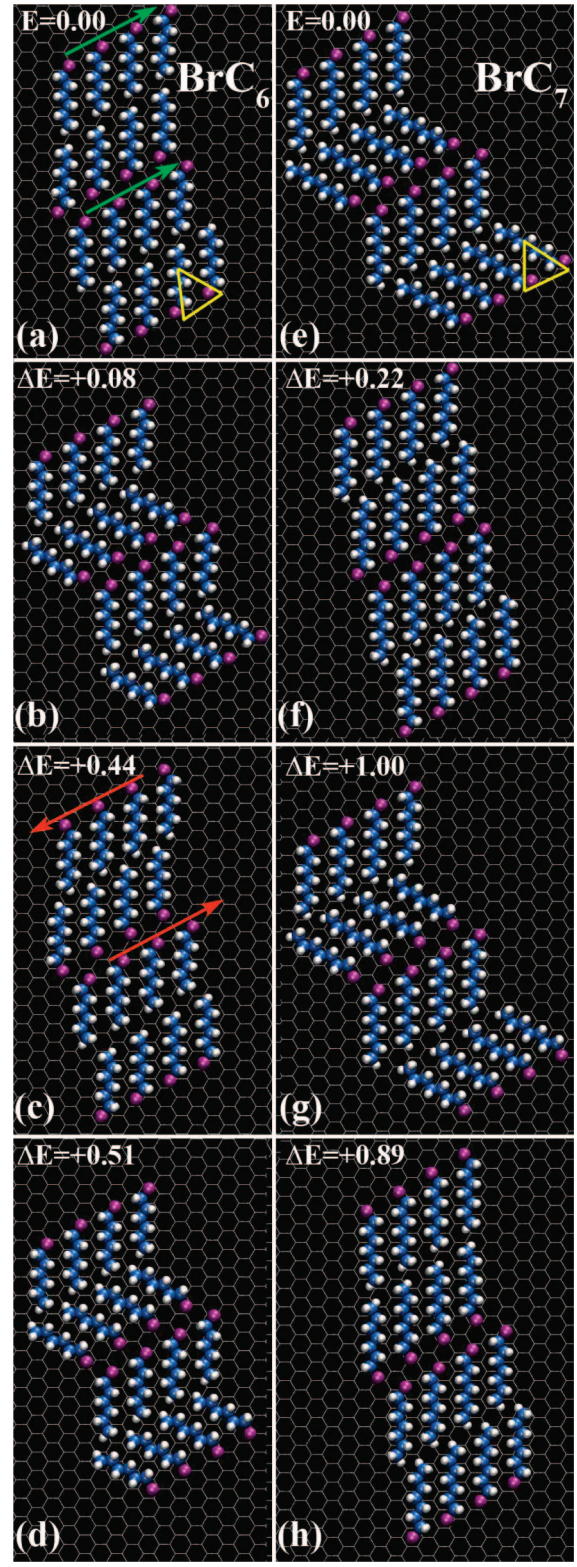

Figure 2. Minimized structures of (a−d) 1-bromohexane and (e−h) 1-bromoheptane molecules on graphite in vacuum. The C, H, and Br atoms are colored blue, white, and purple, respectively. The stable packing configurations (a, b, e, f) are those in which the condition for close-packing (Br interdigitated between two H atoms as indicated by the yellow triangle) is satisfied. Energies are given in kcal/mol/molecule relative to the corresponding minimum energy configurations of BrC_6 (a) in the left column and BrC_7 (e).

TABLE 2: Breakdown of the Potential Energy into Its Component Parts for Each Calculated Structure Shown in Figure 2

	BrC_6 (a)[b] E=0.00	BrC_6 (b)[b] ΔE =+0.08	BrC_6 (c)[b] ΔE =+0.44	BrC_6 (d)[b] ΔE =+0.51	BrC_7 (e)[b] E=0.00	BrC_7 (f)[b] ΔE =+0.22	BrC_7 (g)[b] ΔE =+0.89	BrC_7 (h)[b] ΔE =+1.00
total potential energy [a]	−21.0694	−20.9856	−20.6277	−20.5626	−24.1593	−23.9411	−23.2700	−23.1593
stretch	0.03300	0.033688	0.041125	0.034188	0.051250	0.054375	0.048375	0.045875
bend	0.43625	0.427375	0.423813	0.428375	0.514875	0.523625	0.526938	0.519750
torsion	0.086625	0.089000	0.087313	0.087688	0.091500	0.090813	0.093688	0.092438
Lennard−Jones	−4.39244	−4.32338	−4.25788	−4.33719	−5.34269	−5.30288	−4.87225	−4.79825
Steele	−18.5566	−18.4922	−18.4633	−18.3196	−20.9954	−20.8651	−20.8577	−20.8167
electrostatic	1.891188	2.02975	2.542563	2.520063	2.296313	2.149500	2.793625	2.800875
image charge	−0.56744	−0.74988	−1.00138	−0.97619	−0.77519	−0.59163	−1.00263	−1.00325

[a] The total potential energy of each structure is given in kcal/mol/molecule. [b] The corresponding structures are shown in Figure 2a−h.

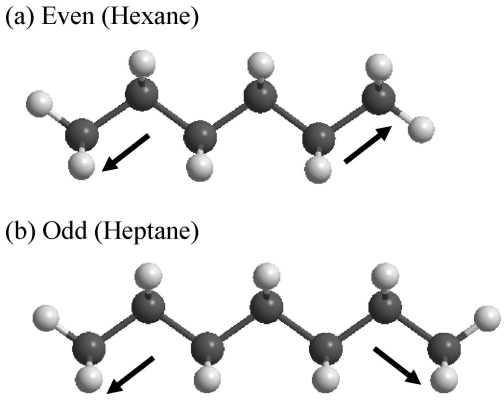

Figure 3. Ball and stick models showing the relative orientations of the terminal vectors for (a) even- and (b) odd-length *n*-alkanes.

correspondingly small fluctuations about its equilibrium distance with respect to the fixed atoms of the graphite lattice. The Br atom lies approximately in the same plane as the carbon backbone atoms of the alkane chain since its van der Waals radius is similar to that of carbon. On the other hand, the energy terms of the torsion angles involving the terminal Br atoms are only 1.33 times as large as those involving the terminal hydrogen atoms. The entire molecule is expected to be oriented parallel to the graphite surface with a 0° angle between the planes containing the carbon backbone, the terminal bromine group, and the substrate.

STM topographic images of the monolayer formed by BrC_7 on graphite under low-temperature, UHV conditions (Figure 1c, d) differ from those observed for BrC_6. The BrC_7 molecules adopt a herringbone assembly in which there is a $60 \pm 3°$ angle between the lamella and molecular backbone axes (labeled ϕ in Figure 1d). A Moiré pattern is clearly observed for the BrC_7 monolayer as a result of the lack of exact commensurability between the monolayer and the underlying graphite lattice along the lamella axis. The Moiré pattern in the STM image repeats every 3.64 nm. Assuming an intermolecular distance ($b_\perp$) of 0.44 nm, consistent with the experimental spacing in BrC_6 and the theoretical values obtained for both 1-bromoalkanes, the period of the interference pattern is eight molecules. The double lamella spacing of $a = 1.82$ nm is comparable to the sum of twice the calculated length of a single BrC_7 molecule (0.9 nm) and the van der Waals diameter of a carbon atom, after accounting for the 60° angle of both molecules in the row. The STM images and theoretical analysis confirm that the molecules are in the favorable all-*trans* configuration and are lying flat on the graphite, as in the case of BrC_6. The BrC_7 molecules pack in a head-to-head configuration, where individual bromine atoms are clearly observed in the STM images as bright circles (Figure 1c, d). The theoretical analysis of the monolayer structure shows that, unlike the BrC_6 monolayer, the bromine atoms from neighboring lamella are oriented in the same direction (Figure 2e). In both cases, the bromine atoms are orientated such that they interdigitate or nest between the two hydrogen atoms of a neighboring chain (yellow triangles in Figure 2).

A defect in the self-assembled monolayer of BrC_7 is displayed in the upper middle portion of the STM image of BrC_7 (Figure 1c) in which bromine atoms are observed both in the dark methyl trough, as well as in the bright stripe where the bromine atoms typically appear. This alternating pattern of bromine atoms within a lamella is consistent with a head-to-tail type packing defect. Such packing defects are uncommon in the 1-bromoalkane monolayers, in keeping with their higher total energy as predicted by the theoretical analysis of bromine head-to-tail type structures for BrC_6.[17]

The theoretical analysis of 1-bromohexane and 1-bromoheptane at the graphite-vacuum interface indicates that the observed odd/even structural alternation is driven by the optimization of close-packing. Figure 2 shows the results of energy minimizations for several representative BrC_6 (left column) and BrC_7 (right column) configurations for both the herringbone and the ∼60° lamella-molecular backbone morphologies. The analysis was performed by systematic variation of all possible orientations of the head-to-head and tail-to-tail groups with respect to each other. The orientations in the top four configurations (Figure 2a, b, e and f) were determined to be the most stable. These configurations are characterized by the nesting of the bromine atoms in between hydrogen atoms of the neighboring chain (yellow triangles). The total potential energy for all the configurations with nested bromines was found to be consistently lower than the corresponding configurations for which the bromine atoms of one chain are not embedded between hydrogen atoms of the nearest neighbor chain. The favorable tail-to-tail orientations are such that bromine atoms from alternate lamellae point along the same direction (green arrows in Figure 2a). The bottom four configurations (Figure 2c, d, g, h) depict a representative set of morphologies for which the total potential energy is higher. The molecules in a subset of the lamellae are flipped about the backbone axis relative to the corresponding top four panels in Figure 2. Notice in Figure 2c, for example, that the bromine atoms in the second from bottom lamella are no longer nested between hydrogen atoms of the neighboring chains. In addition, the orientations of the Br atoms from alternate lamellae are not oriented along the same direction (red arrows in Figure 2c).

For BrC_6, it was previously determined using the OPLS united-atom (UA) force field that the minimum energy configuration is one in which the molecules align with ∼60° lamella-molecular backbone angles, and bromine end-groups from neighboring lamellae are oriented in opposite directions relative to each other.[17] This result has been duplicated here with the OPLS all-atom (AA) force field. Although the unit cell

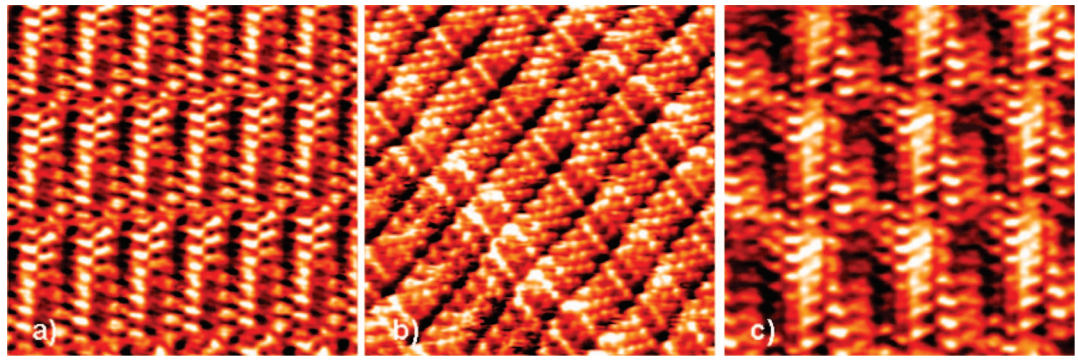

Figure 4. UHV-STM Images of *n*-alkanes on graphite at 80 K (a) hexane: 12 nm × 12 nm, +1.9 V, 90 pA, 7 lines/s, active drift control, (b) heptane: 10 nm × 10 nm, +1.9 V, 90 pA, 7 lines/s, active drift control, and (c) octane: 7.5 nm × 7.5 nm, +1.75 V, 150 pA, 6 lines/s, no drift control. All images have been FFT filtered slightly to sharpen their features without inducing distortion.

parameters (Table 1) and absolute potential energy (Table 2) are altered somewhat, the net result is the same (Figure 2a). Since hydrogen atoms are treated explicitly in the AA force field, small changes in the packing structures are not surprising. The AA force field is expected to provide a more realistic description of the packing structures.

In further agreement with the experimental findings, the most stable configuration for BrC_7 is the herringbone morphology (Figure 2e). The breakdown of the total potential energy (Table 2) provides an interesting interpretation for the alternation of the structures as a function of the odd/even number of backbone atoms. The choice of the herringbone pattern for BrC_7 and the nonherringbone pattern for BrC_6 is seen to be driven by the Lennard−Jones and Steele contributions to the potential energy (compare column a with b, and column e with f in Table 2). The relative electrostatic and image charge contributions are, on the other hand, independent of whether the chain-length is odd or even. The electrostatic contribution favors the herringbone morphology whereas, the image charge contribution favors the nonherringbone morphologies for both BrC_6 and BrC_7. This suggests that the odd/even effect is governed by the optimization of close-packing, in agreement with previous studies of the self-assembly of *n*-alkanes and alcohols. We note that the variation in the energies between the different morphologies (Table 2) is relatively small. The differences, however, are expressed in terms of potential energy per chain and as such can add up significantly for large domain morphologies. In the case of 1-bromoalkanes, the presence of the highly polarizable bromine headgroup and the C−Br bond dipole introduce additional subtleties concerning the conditions for which the close packing and commensurability are optimized relative to the simpler *n*-alkanes.

We have also attempted to minimize a few putative initial 90° configurations of BrC_6, however, all the configurations examined have converted rapidly to a 60° configuration, even at temperatures as low as 5K. The rapid 90°-to-60° transition indicates that the basin of the potential energy surface (PES) about the minimum energy configuration of the 90° morphology is very narrow; the corresponding basin about the minimum energy of the 60° configuration, on the other hand, must be much broader. For BrC_{20} (1-bromoeicosane), we have also determined that the basin of the potential energy landscape about the minimum energy of the 90° configuration under vacuum conditions is very narrow.[21] For the lowest energy 90° and 60° BrC_{20} morphologies, the difference in their total potential energy is calculated to be negligible.[21] Nevertheless, the 90° configuration, with its very narrow basin, is less likely to be observed experimentally for the self-assembly process under deposition from vacuum, in agreement with the STM experiment. The origin of the narrow PES basin about the 90° minimum energy configuration is due to the unfavorable dipole−dipole alignment of the Br head groups between opposing lamellae.[17] The high polarizability of the Br atoms may also play a role since the rectangular head-to-head formation does not restrict the interpenetration of Br atoms from opposing lamellae. For the 60° formation, on the other hand, opposing Br atoms are stabilized through confinement in between hydrogen atoms of neighboring chains.[21]

Discussion

A systematic alternation is observed in the self-assembled morphologies of *n*-alkanes and their derivatives in two dimensions as a function of chain length. The structural alternation is due to the fact that close-packing is achieved in different ways depending on the relative orientations of the terminal backbone vectors. For even-length *n*-alkanes, the terminal vectors are aligned in parallel with respect to each other (Figure 3a) whereas for odd-length *n*-alkanes, they are not (Figure 3b). The odd/even effect gives rise to two different morphologies of *n*-alkane monolayers on graphite: herringbone configurations for the even-length species and rectangular (90° lamella-molecular backbone angle) configurations for the odd-length ones.

STM images of these morphologies are displayed in Figure 4 (for hexane, heptane, and octane adsorbed on graphite at 80 K under vacuum) and serve as a comparison for the 1-bromoalkane structures. The monolayers show the expected morphologies, namely, even-length hexane and octane form herringbone lamella-molecular backbone structures and the odd-length heptane forms a nearly rectangular lamella-molecular backbone structure, in general agreement with the diffraction-based predictions.[45,46] The molecules are assumed to lie flat on the graphite based on our 1-bromoalkane simulations, as described above (see Results section). A strong Moiré effect is observed along both the lamella axis and across lamellae for each *n*-alkane. These patterns indicate that the chains are not in perfect registry with the graphite lattice. Simulations of hexane on graphite confirm that the average interchain distance, 4.4 Å, is slightly larger than the corresponding graphite spacing, 4.26 Å. The mismatch occurs while the chains are approximately close-packed at 80 K. Results from calculations on long 1-bromoalkanes indicate that a compressed intermolecular spacing (~3.8 Å) can be achieved by rotating the molecular backbones with respect to the graphite surface such that they lie perpendicular to the surface, with the carbon atoms of neighboring methylene units at different heights above the

graphite surface.[83] Despite a more tightly packed monolayer structure, the net result is higher total potential energy for these perpendicular configurations due to less favorable dispersion interactions between the molecules and the graphite surface as compared to the flat (parallel) configuration. Extrapolating from the conclusions of our theoretical studies above on 1-bromoalkanes, the relative orientations of the terminal vectors as a function of chain length (Figure 3) are expected to alter the morphology in the simple *n*-alkanes so as to optimize as much as possible both close-packing and commensurability. The odd/even structural alternation is no longer observed in 2D crystals of very long *n*-alkanes, where only rectangular structures are observed.[2−4] This is expected since the effect of the relative orientation of the terminal backbone vectors should become negligible above some critical chain length.[84] According to the 2DSD compiled by Matzger and co-workers,[1] a change in monolayer morphology from oblique to rectangular occurs for the *n*-alkanes between tetracosane ($C_{24}H_{50}$) and octacosane ($C_{28}H_{58}$), respectively, at the liquid−graphite interface.

In the case of the 1-bromoalkanes, 1-bromohexane and 1-bromoheptane behave as an odd- and even-length *n*-alkane, respectively, because the bromine atom acts effectively as an extension of the alkane backbone. The simulations predict that the height of the bromine atom above the graphite surface is largely fixed by the polarizability of the bromine atom such that the terminal carbon−bromine vector is essentially parallel to the graphite axis at 80 K. The analogy between the 1-bromoalkanes and the *n*-alkanes, however, is incomplete since the lamella-backbone angle of 1-bromohexane (60°) differs from that of heptane (90°). In addition, the bromine atoms orient in a head-to-head configuration, which initially seems counter intuitive, yet is favorable due to electrostatic and dispersion interactions between the bromine atoms from opposite lamellae. These same interactions are also responsible for the choice of the 60° morphology for BrC_6 since the minimum energy configuration of the 90° form is likely to be kinetically inaccessible under vacuum conditions. The relative orientation of the bromine atoms from opposite lamellae is governed by the condition for interdigitation - the nesting of Br in between hydrogen atoms of nearest neighbor chains for both the odd- and even-length 1-bromoalkanes (yellow triangles in Figure 2a and e). Interestingly, this condition results in different dipole−dipole configurations for the bromine head groups in the case of the odd- and even-length 1-bromoalkanes.

Conclusions

The relative orientation of the terminal vectors (odd/even effect) dictates the observed alternation in the 2D packing structures for *n*-alkane derivatives on graphite. The analogies and subtle differences that are observed for the odd/even packing effect of short 1-bromoalkanes versus that of short *n*-alkanes are due to the dual role played by the bromine atom as an extension of the alkane backbone and as a polarizable headgroup. Investigations into the driving forces for self-assembly of other types of end-groups, such as those presented by alcohols and carboxylic acids with strong, directional hydrogen-bonding interactions, are presently being explored.

Acknowledgment. This work was supported by the National Science Foundation through Grants No. CHE-07-01483 (to G.W.F.) and CHE-06-13401 (to B.J.B.), the NSEC Program (CHE-06-41523) and by the New York State Office of Science, Technology, and Academic Research (NYSTAR). G.M.F. thanks the Henry Luce Foundation for support in the form of a Clare Boothe Luce Assistant Professorship in Chemistry.

References and Notes

(1) Plass, K. E.; Grzesiak, A. L.; Matzger, A. J. Molecular packing and symmetry of two-dimensional crystals. *Acc. Chem. Res.* **2007**, *40* (4), 287–293.

(2) McGonigal, G. C.; Bernhardt, R. H.; Thomson, D. J. Imaging Alkane Layers at the Liquid Graphite Interface with the Scanning Tunneling Microscope. *Appl. Phys. Lett.* **1990**, *57* (1), 28–30.

(3) McGonigal, G. C.; Bernhardt, R. H.; Yeo, Y. H.; Thomson, D. J. Observation of Highly Ordered, 2-Dimensional *n*-Alkane and *n*-Alkanol Structures on Graphite. *J. Vac. Sci. Technol. B* **1991**, *9* (2), 1107–10.

(4) Rabe, J. P.; Buchholz, S. Commensurability and mobility in 2-dimensional molecular-patterns on graphite. *Science* **1991**, *253* (5018), 424–7.

(5) Cyr, D. M.; Venkataraman, B.; Flynn, G. W.; Black, A.; Whitesides, G. M. Functional Group Identification in Scanning Tunneling Microscopy of Molecular Adsorbates. *J. Phys. Chem.* **1996**, *100* (32), 13747–13759.

(6) Watel, G.; Thibaudau, F.; Cousty, J. Direct Observation of Long-Chain Alkane Bilayer Films on Graphite by Scanning Tunneling Microscopy. *Surf. Sci.* **1993**, *281* (1−2), L297–L302.

(7) Wan, L. J. Fabricating and Controlling Molecular Self-Organization at Solid Surfaces: Studies by Scanning Tunneling Microscopy. *Acc. Chem. Res.* **2006**, *39* (5), 334–342.

(8) De Feyter, S.; De Schryver, F. C. Self-Assembly at the Liquid/Solid Interface: STM Reveals. *J. Phys. Chem. B* **2005**, *109* (10), 4290–4302.

(9) De Feyter, S.; De Schryver, F. C. Two-Dimensional Supramolecular Self-Assembly Probed by Scanning Tunneling Microscopy. *Chem. Soc. Rev.* **2003**, *32* (3), 139–150.

(10) De Feyter, S.; Gesquiere, A.; Abdel-Mottaleb, M. M.; Grim, P. C. M.; De Schryver, F. C.; Meiners, C.; Sieffert, M.; Valiyaveettil, S.; Mullen, K. Scanning Tunneling Microscopy: a Unique Tool in the Study of Chirality, Dynamics, and Reactivity in Physisorbed Organic Monolayers. *Acc. Chem. Res.* **2000**, *33* (8), 520–531.

(11) Giancarlo, L. C.; Flynn, G. W. Raising Flags: Applications of Chemical Marker Groups to Study Self-Assembly, Chirality, and Orientation of Interfacial Films by Scanning Tunneling Microscopy. *Acc. Chem. Res.* **2000**, *33* (7), 491–501.

(12) Giancarlo, L. C.; Flynn, G. W. Scanning Tunneling and Atomic Force Microscopy Probes of Self-Assembled, Physisorbed Monolayers: Peeking at the Peaks. *Annu. Rev. Phys. Chem.* **1998**, *49*, 297–336.

(13) Cyr, D. M.; Venkataraman, B.; Flynn, G. W. STM Investigations of Organic Molecules Physisorbed at the Liquid−Solid Interface. *Chem. Mater.* **1996**, *8* (8), 1600–1615.

(14) Frommer, J. Scanning Tunneling Microscopy and Atomic Force Microscopy in Organic Chemistry. *Angew. Chem., Int. Ed. Engl.* **1992**, *31* (10), 1298–1328.

(15) Tao, F.; Bernasek, S. L. Understanding Odd−Even Effects in Organic Self-Assembled Monolayers. *Chem. Rev.* **2007**, *107* (5), 1408–1453.

(16) Dobrin, S.; Harikumar, K. R.; Polanyi, J. C. STM Study of the Conformation and Reaction of Long-Chain Haloalkanes at Si(111)-7 × 7. *J. Phys. Chem. B* **2006**, *110* (15), 8010–8018.

(17) Müller, T.; Werblowsky, T. L.; Florio, G. M.; Berne, B. J.; Flynn, G. W. Ultra-high Vacuum Scanning Tunneling Microscopy and Theoretical Studies of 1-Halohexane Monolayers on Graphite. *Proc. Natl. Acad. Sci. U.S.A.* **2005**, *102* (15), 5315–5322.

(18) Lackinger, M.; Griessl, S.; Heckl, W. A.; Hietschold, M.; Flynn, G. W. Self-Assembly of Trimesic Acid at the Liquid−Solid Interface - a Study of Solvent-Induced Polymorphism. *Langmuir* **2005**, *21* (11), 4984–4988.

(19) Kim, K. B.; Plass, K. E.; Matzger, A. J. Conformational Pseudopolymorphism and Orientational Disorder in Two-Dimensional Alkyl Carbamate Crystals. *Langmuir* **2005**, *21* (2), 647–655.

(20) Plass, K. E.; Kim, K.; Matzger, A. J. Two-Dimensional Crystallization: Self-Assembly, Pseudopolymorphism, and Symmetry-Independent Molecules. *J. Am. Chem. Soc.* **2004**, *126* (29), 9042–9053.

(21) Ilan, B.; Florio, G. M.; Werblowsky, T. L.; Müller, T.; Hybertsen, M. S.; Berne, B. J.; Flynn, G. W. Solvent Effects in the Self-Assembly of 1-Bromoeicosane on Graphite. Part II Theory. Submitted for publication, **2008**.

(22) Herwig, K. W.; Matthies, B.; Taub, H. Solvent Effects on the Monolayer Structure of Long *n*-alkane Molecules Adsorbed on Graphite. *Phys. Rev. Lett.* **1995**, *75* (17), 3154–3157.

(23) Florio, G. M.; Klare, J. E.; Pasamba, M. O.; Werblowsky, T. L.; Hyers, M.; Berne, B. J.; Hybertsen, M. S.; Nuckolls, C.; Flynn, G. W. Frustrated Ostwald Ripening in Self-Assembled Monolayers of Cruciform π-Systems. *Langmuir* **2006**, *22* (24), 10003–10008.

(24) Florio, G. M.; Werblowsky, T. L.; Müller, T.; Berne, B. J.; Flynn, G. W. Self-Assembly of Small Polycyclic Aromatic Hydrocarbons on Graphite: a Combined Scanning Tunneling Microscopy and Theoretical Approach. *J. Phys. Chem. B* **2005**, *109* (10), 4520–4532.

(25) Abdel-Mottaleb, M. M. S.; Gotz, G.; Kilickiran, P.; Bauerle, P.; Mena-Osteritz, E. Influence of Halogen Substituents on the Self-Assembly of Oligothiophenes - A Combined STM and Theoretical Approach. *Langmuir* **2006**, *22* (4), 1443–1448.

(26) Werblowsky, T. L. Self-Assembly at the Theoretical−Experimental Interface: Computer Simulations of Organic Systems on Graphite, Ph.D. thesis, Columbia University, New York, 2003.

(27) Yin, S.; Wang, C.; Qiu, X.; Xu, B.; Bai, C.-L. Theoretical Study of the Effects of Intermolecular Interactions in Self-Assembled Long-Chain Alkanes Adsorbed on Graphite Surface. *Surf. Interface Anal.* **2001**, *32* (1), 248–52.

(28) Kannappan, K.; Werblowsky, T. L.; Rim, K. T.; Berne, B. J.; Flynn, G. W. An Experimental and Theoretical Study of the Formation of Nanostructures of Self-Assembled Cyanuric Acid through Hydrogen Bond Networks on Graphite. *J. Phys. Chem. B* **2007**, *111* (24), 6634–6642.

(29) Groszek, A. J. Selective Adsorption at Graphite/Hydrocarbon Interfaces. *Proc. R. Soc. London, Ser. A* **1970**, *314* (1519), 473–498.

(30) Findenegg, G. H.; Liphard, M. *Carbon* **1987**, *25*, 119.

(31) Müller, T.; Flynn, G. W.; Mathauser, A. T.; Teplyakov, A. V. Temperature-Programmed Desorption Studies of *n*-Alkane Derivatives on Graphite: Desorption Energetics and the Influence of Functional Groups on Adsorbate Self-Assembly. *Langmuir* **2003**, *19* (7), 2812–2821.

(32) Paserba, K. R.; Gellman, A. J. Kinetics and Energetics of Oligomer Desorption from Surfaces. *Phys. Rev. Lett.* **2001**, *86* (19), 4338–41.

(33) Paserba, K. R.; Gellman, A. J. Effects of Conformational Isomerism on the Desorption Kinetics of *n*-Alkanes from Graphite. *J. Chem. Phys.* **2001**, *115* (14), 6737–51.

(34) Espeau, P.; Reynolds, P. A.; Dowling, T.; Cookson, D.; White, J. W. X-ray Diffraction from Layers of *n*-Alkanes Adsorbed on Graphite. *J. Chem. Soc., Faraday Trans.* **1997**, *93* (17), 3201–3208.

(35) Fuhrmann, D.; Criswell, L.; Mo, H.; Volkmann, U. G.; Herwig, K. W.; Taub, H.; Hansen, F. Y. Diffusive Motion in Model Soft Matter Systems: Quasielastic Neutron Scattering Study of Short- and Intermediate-Length Alkane Layers. *Physica B* **2000**, *276*, 345–346.

(36) Fuhrmann, D.; Graham, A. P.; Criswell, L.; Mo, H.; Matthies, B.; Herwig, K. W.; Taub, H. Effects of Chain Branching on the Monolayer Structure of Alkanes at Interfaces: a Neutron and Helium Atom Scattering Study. *Surf. Sci.* **2001**, *482*, 77–82.

(37) Gilbert, E.; Reynolds, P.; White, J. Application of Small-Angle Scattering to the Study of Graphite-Adsorbed Hydrocarbons. *J. Appl. Crystallogr.* **2000**, *33* (1), 744–748.

(38) Herwig, K. W.; Wu, Z.; Dai, P.; Taub, H.; Hansen, F. Y. Quasielastic Neutron Scattering and Molecular Dynamics Simulation Studies of the Melting Transition in Butane and Hexane Monolayers Adsorbed on Graphite. *J. Chem. Phys.* **1997**, *107* (13), 5186–5196.

(39) Kraack, H.; Ocko, B. M.; Pershan, P. S.; Sloutskin, E.; Deutsch, M. Langmuir Films of Normal-Alkanes on the Surface of Liquid Mercury. *J. Chem. Phys.* **2003**, *119* (19), 10339–10349.

(40) Krim, J.; Suzanne, J.; Shechter, H.; Wang, R.; Taub, H. A LEED and Neutron Diffraction Study of Hexane Adsorbed on Graphite in the Monolayer Range: Uniaxial Commensurate Incommensurate Transition. *Surf. Sci.* **1985**, *162*, 446–51.

(41) Kruchten, F.; Knorr, K.; Volkmann, U. G.; Taub, H.; Hansen, F. Y.; Matthies, B.; Herwig, K. W. Ellipsometric and Neutron Diffraction Study of Pentane Physisorbed on Graphite. *Langmuir* **2005**, *21* (16), 7507–7512.

(42) Nozaki, K. X-ray and Thermal Studies on the Crystalline Phases of Normal Alkanethiols n-$C_nH_{2n+1}SH$ (n = 18, 19, 22, 23, 24). *J. Mater. Sci.* **2006**, *41* (12), 3935–3946.

(43) Ocko, B. M.; Wu, X. Z.; Sirota, E. B.; Sinha, S. K.; Gang, O.; Deutsch, M. Surface Freezing in Chain Molecules: Normal Alkanes. *Phys. Rev. E: Stat. Phys.* **1997**, *55* (3), 3164–3182.

(44) Wu, Z.; Ehrlich, S. N.; Matthies, B.; Herwig, K. W.; Dai, P. C.; Volkmann, U. G.; Hansen, F. Y.; Taub, H. Growth of *n*-Alkane Films on a Single-Crystal Substrate. *Chem. Phys. Lett.* **2001**, *348* (3−4), 168–174.

(45) Arnold, T.; Dong, C. C.; Thomas, R. K.; Castro, M. A.; Perdigon, A.; Clarke, S. M.; Inaba, A. The Crystalline Structures of the Odd Alkanes Pentane, Heptane, Nonane, Undecane, Tridecane and Pentadecane Monolayers Adsorbed on Graphite at Submonolayer Coverages and from the Liquid. *Phys. Chem. Chem. Phys.* **2002**, *4* (14), 3430–3435.

(46) Arnold, T.; Thomas, R. K.; Castro, M. A.; Clarke, S. M.; Messe, L.; Inaba, A. The Crystalline Structures of the Even Alkanes Hexane, Octane, Decane, Dodecane and Tetradecane Monolayers Adsorbed on Graphite at Submonolayer Coverages and from the Liquid. *Phys. Chem. Chem. Phys.* **2002**, *4* (2), 345–351.

(47) Becker, K. E.; Fichthorn, K. A. Accelerated Molecular Dynamics Simulation of the Thermal Desorption of *n*-Alkanes from the Basal Plane of Graphite. *J. Chem. Phys.* **2006**, *125* (18).

(48) Fodi, B.; Hentschke, R. Molecular Dynamics Simulation of a Binary Hydrocarbon Mixture near an Adsorbing Wall: Benzene/*n*-Heptane on Graphite. *Langmuir* **1998**, *14* (2), 429–437.

(49) Peters, G. H. The Molecular Dynamics Simulations of the Melting of a Hexane Bilayer. *Surf. Sci.* **1996**, *347* (1−2), 169–181.

(50) Pint, C. L. Different Melting Behavior in Pentane and Heptane Monolayers on Graphite: Molecular Dynamics Simulations. *Phys. Rev. B: Condens. Matter.* **2006**, *73* (4).

(51) Pint, C. L.; Roth, M. W.; Wexler, C. Behavior of Hexane on Graphite at Near-Monolayer Densities: Molecular Dynamics Study. *Phys. Rev. B: Condens. Matter.* **2006**, *73* (8).

(52) Yang, H.; Li, Z. S.; Lu, Z. Y.; Sun, C. C. Molecular Dynamics Simulations Study on the Melting Process of *n*-Heptane Layer(s) Adsorbed on the Graphite (001) Surface. *Surf. Sci.* **2006**, *600* (6), 1213–1220.

(53) Krishnan, M.; Balasubramanian, S. Phase Behaviour of Ultrathin Crystalline *n*-Heptane Films on Graphite: An Atomistic Simulation Study. *Phys. Chem. Chem. Phys.* **2005**, *7* (9), 2044–2052.

(54) Krishnan, M.; Balasubramanian, S. *n*-Heptane under Pressure: Structure and Dynamics from Molecular Simulations. *J. Phys. Chem. B* **2005**, *109* (5), 1936–1946.

(55) Krishnan, M.; Balasubramanian, S.; Clarke, S. Structure of Solid Monolayers and Multilayers of *n*-Hexane on Graphite. *Proc. Ind. Acad. Sci.−Chem. Sci.* **2003**, *115* (5−6), 663–677.

(56) Krishnan, M.; Balasubramanian, S.; Clarke, S. An Atomistic Simulation Study of a Solid Monolayer and Trilayer of *n*-Hexane on Graphite. *J. Chem. Phys.* **2003**, *118* (11), 5082–5086.

(57) Pint, C. L. Simulations of the Chain Length Dependence of the Melting Mechanism in Short-Chain *n*-Alkane Monolayers on Graphite. *Surf. Sci.* **2006**, *600* (4), 921–932.

(58) Pint, C. L.; Roth, M. W. Simulated Effects of Odd-Alkane Impurities in a Hexane Monolayer on Graphite. *Phys. Rev. B: Condens. Matter.* **2006**, *73* (11).

(59) Hansen, F. Y.; Newton, J. C.; Taub, H. Molecular-Dynamics Studies of the Melting of Butane and Hexane Monolayers Adsorbed on the Basal-Plane Surface of Graphite. *J. Chem. Phys.* **1993**, *98* (5), 4128–4141.

(60) Roth, M. W.; Pint, C. L.; Wexler, C. Phase Transitions in Hexane Monolayers Physisorbed onto Graphite. *Phys. Rev. B: Condens. Matter.* **2005**, *71* (15), 155427.

(61) Connolly, M. J.; Roth, M. W.; Gray, P. A.; Wexler, C. Explicit Hydrogen Molecular Dynamics Simulations of Hexane Deposited onto Graphite at Various Coverages. *Langmuir* **2008**, *24* (7), 3228–3234.

(62) Hansen, F. Y.; Taub, H. The Mechanism of Melting in Monolayer Films of Short and Intermediate-Length *n*-Alkanes Adsorbed on Graphite. *Inorg. Mater.* **1999**, *35* (6), 586–592.

(63) Morishige, K.; Kato, T. Chain-Length Dependence of Melting of *n*-Alcohol Monolayers Adsorbed on Graphite: *n*-Hexanol, *n*-Heptanol, *n*-Octanol, and *n*-Nonanol. *J. Chem. Phys.* **1999**, *111* (15), 7095–7102.

(64) Morishige, K.; Takami, Y.; Yokota, Y. Structures of Alkanes and Alkanols Adsorbed on Graphite in Solution: Comparison with Scanning-Tunneling-Microscopy Images. *Phys. Rev. B* **1993**, *48* (11), 8277–81.

(65) Zhang, H. M.; Yan, J. W.; Xie, Z. X.; Mao, B. W.; Xu, X. Self-Assembly of Alkanols on Au(111) Surfaces. *Chem.-Eur. J.* **2006**, *12* (15), 4006–4013.

(66) Bickerstaffe, A. K.; Cheah, N. P.; Clarke, S. M.; Parker, J. E.; Perdigon, A.; Messe, L.; Inaba, A. The Crystalline Structures of Carboxylic Acid Monolayers Adsorbed on Graphite. *J. Phys. Chem. B* **2006**, *110* (11), 5570–5575.

(67) Hibino, M.; Sumi, A.; Tsuchiya, H.; Hatta, I. Microscopic Origin of the Odd−Even Effect in Monolayer of Fatty Acids Formed on a Graphite Surface by Scanning Tunneling Microscopy. *J. Phys. Chem. B* **1998**, *102* (23), 4544–4547.

(68) Fang, H. B.; Giancarlo, L. C.; Flynn, G. W. Packing of $Br(CH_2)(10)COOH$ and $Br(CH_2)(11)COOH$ on Graphite: An Odd−Even Length Effect Observed by Scanning Tunneling Microscopy. *J. Phys. Chem. B* **1998**, *102* (38), 7421–7424.

(69) Wintgens, D.; Yablon, D. G.; Flynn, G. W. Packing of $HO(CH_2)(14)COOH$ and $HO(CH_2)(15)COOH$ on Graphite at the Liquid−Solid Interface Observed by Scanning Tunneling Microscopy: Methylene Unit Direction of Self-Assembly Structures. *J. Phys. Chem. B* **2003**, *107* (1), 173–179.

(70) Yablon, D. G.; Wintgens, D.; Flynn, G. W. Odd/Even Effect in Self-Assembly of Chiral Molecules at the Liquid−Solid Interface: An STM Investigation of Coadsorbate Control of Self-Assembly. *J. Phys. Chem. B* **2002**, *106* (21), 5470–5475.

(71) Messe, L.; Perdigon, A.; Clarke, S. M.; Castro, M. A.; Inaba, A. Layer-by-Layer Surface Freezing of Linear Alcohols at the Graphite/Liquid Interface. *J. Colloid Interface Sci.* **2003**, *266* (1), 19–27.

(72) Florio, G. M.; Meier, J.; Campanelli, J. S.; Müller, T. 1-Bromononadecane. Unpublished data.

(73) Xie, Z. X.; Xu, X.; Mao, B. W.; Tanaka, K. Self-Assembled Binary Monolayers of *n*-Alkanes on Reconstructed Au(111) and HOPG Surfaces. *Langmuir* **2002**, *18* (8), 3113–3116.

(74) Tao, F.; Goswami, J.; Bernasek, S. L. Self-Assembly and Odd−Even Effects of Cis-Unsaturated Carboxylic Acids on Highly Oriented Pyrolytic Graphite. *J. Phys. Chem. B* **2006**, *110* (9), 4199–4206.

(75) Stern, H. A.; Xu, H.; Harder, E.; Rittner, F.; Pavese, M.; Berne, B. J. *SIM Molecular Dynamics Program*.

(76) Schlick, T.; Fogelson, A. A Powerful Truncated Newton Method for Potential Energy Minimization. *J. Comput. Chem.* **1987**, *8* (7), 1025–1039.

(77) Martyna, G. J.; Klein, M. L.; Tuckerman, M. Nose−Hoover Chains−The Canonical Ensemble Via Continuous Dynamics. *J. Chem. Phys.* **1992**, *97* (4), 2635–2643.

(78) Bottani, E. J.; Bakaev, V.; Steele, W. A Simulation/Experimental Study of the Thermodynamic Properties of Carbon-Dioxide on Graphite. *Chem. Eng. Sci.* **1994**, *49* (17), 2931–2939.

(79) Steele, W. Molecular-Interactions for Physical Adsorption. *Chem. Rev.* **1993**, *93* (7), 2355–2378.

(80) Steele, W. A. Monolayers of Linear Molecules Adsorbed on the Graphite Basal Plane: Structures and Intermolecular Interactions. *Langmuir* **1996**, *12* (1), 145–153.

(81) Jorgensen, W. L.; Maxwell, D. S.; TiradoRives, J. Development and Testing of the OPLS All-Atom Force Field on Conformational Energetics and Properties of Organic Liquids. *J. Am. Chem. Soc.* **1996**, *118* (45), 11225–11236.

(82) Claypool, C. L.; Faglioni, F.; Matzger, A. J.; Goddard, W. A.; Lewis, N. S. Effects of Molecular Geometry on the STM Image Contrast of Methyl- and Bromo-Substituted Alkanes and Alkanols on Graphite. *J. Phys. Chem. B* **1999**, *103* (44), 9690–9699.

(83) Note that this perpendicular configuration is not one in which the entire molecule is oriented along the surface normal. Furthermore, configurations initiated with out-of-plane tilt angles between 0° (parallel) and 90° (perpendicular) readily relaxed into either the parallel or perpendicular forms.

(84) Taggart, A. M.; Voogt, F.; Clydesdale, G.; Roberts, K. J. An Examination of the Nucleation Kinetics of *n*-alkanes in the Homologous Series $C_{13}H_{28}$ to $C_{32}H_{66}$, and Their Relationship to Structural Type, Associated with Crystallization from Stagnant Melts. *Langmuir* **1996**, *12* (23), 5722–5728.

JP8064689